

## Supplementary information

### **A ratiometric luminescence sensing platform based on lanthanide-based silica nanoparticles for selective and sensitive detection of Fe<sup>3+</sup> and Cu<sup>2+</sup> ions**

Meng-Yao Zhang,<sup>a</sup> Feng-Ying Yi,<sup>a</sup> Qing-Zhong Guo,<sup>a</sup> Fa-Liang Luo,<sup>b</sup> Lan-Jun Liu<sup>\*a, c</sup> and Jun-Fang Guo<sup>\*a</sup>

a. Hubei Key Laboratory of Plasma Chemistry and Advanced Materials, School of Materials Science and Engineering, Wuhan Institute of Technology, Wuhan 430205, China.

b. State Key Laboratory of High-efficiency Utilization of Coal and Green Chemical Engineering, Ningxia University, Yinchuan, 750021, China.

c. School of Civil Engineering and Architecture, Wuhan Institute of Technology, Wuhan 430205, China.

\* Corresponding author: Lanjun Liu; Junfang Guo

E-mail: [witljliu@sina.com](mailto:witljliu@sina.com); [junfangguo@aliyun.com](mailto:junfangguo@aliyun.com)

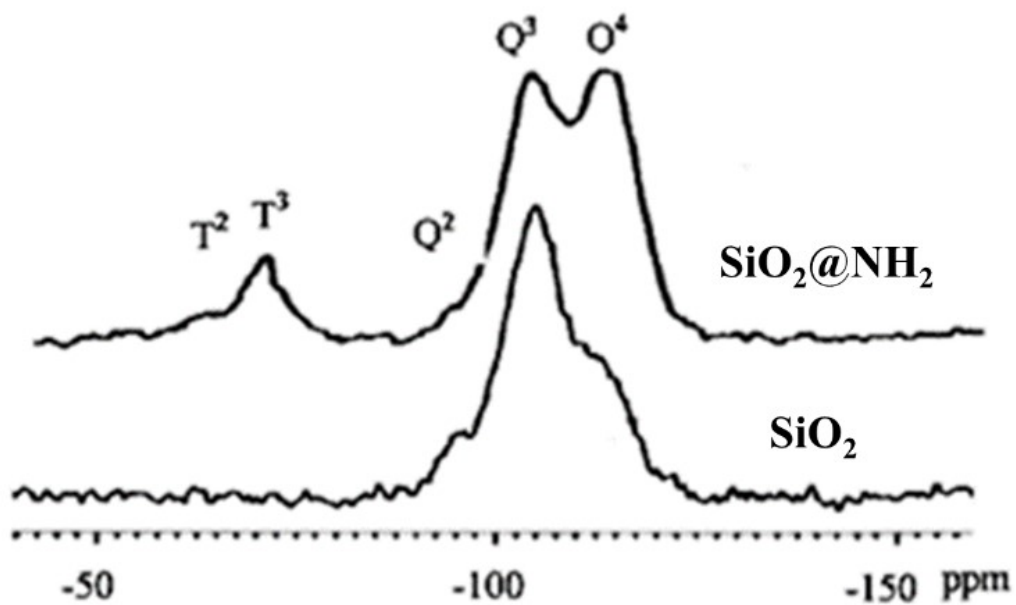


**Fig. S1.**  $^{29}\text{Si}$  MAS NMR spectra of  $\text{SiO}_2$  and  $\text{SiO}_2@\text{NH}_2$  nanoparticles.

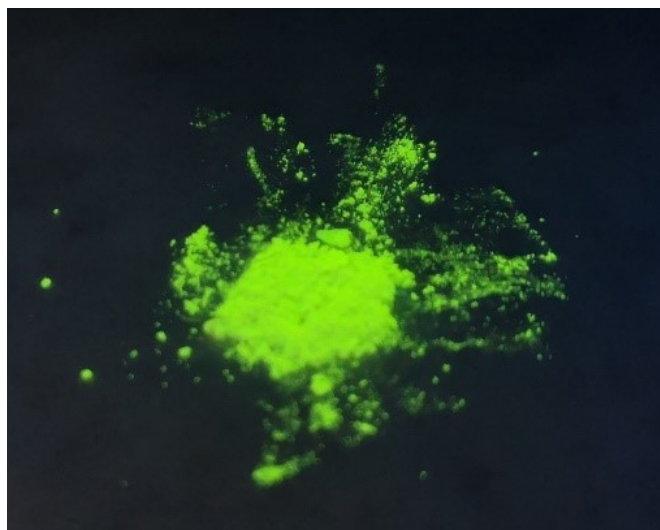


**Fig. S2.** Optical image of  $\text{SiO}_2@\text{Tb}$  nanocomposites under a UV lamp (254 nm).

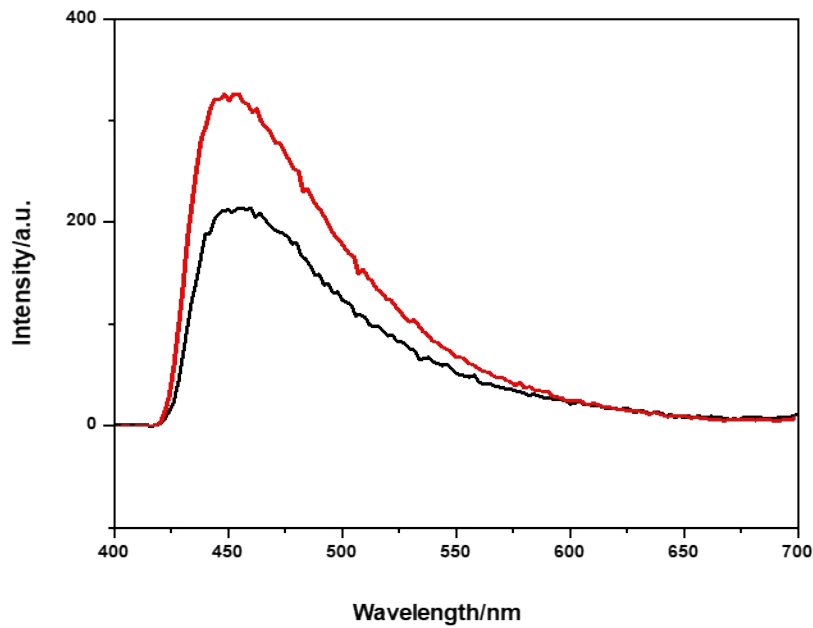


**Fig. S3.** Emission spectra ( $\lambda_{\text{ex}}=237$  nm) of the suspension of  $\text{SiO}_2$  nanoparticles (red) and  $\text{SiO}_2@\text{COOH}$  (black).

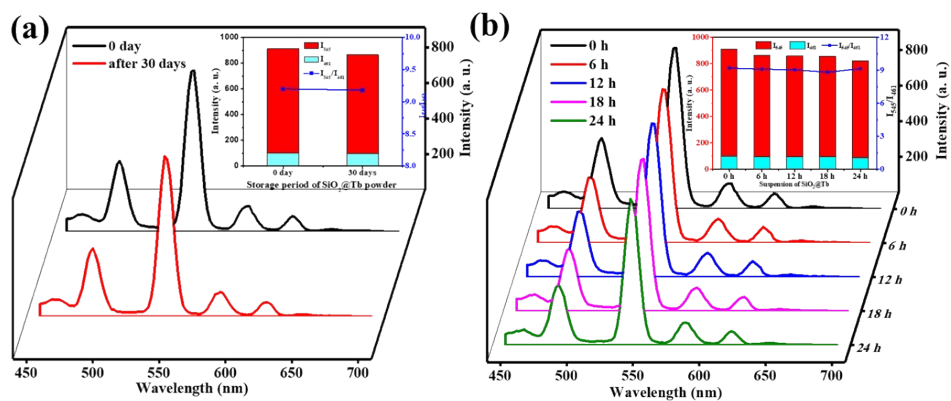


**Fig. S4.** Emission spectra of  $\text{SiO}_2@\text{Tb}$  suspensions ( $\lambda_{\text{ex}}=237$  nm). (a)  $\text{SiO}_2@\text{Tb}$  powder storage 0 or 30 days. (b) the suspension of  $\text{SiO}_2@\text{Tb}$  at 6-hour intervals in a day. (inset: Luminescence intensity of  $\text{SiO}_2@\text{Tb}$  at 545 nm and 461 nm and the corresponding intensity ratio of  $I_{545}/I_{461}$ ). The  $\text{SiO}_2@\text{Tb}$  nanoparticles were immersed into water and ultrasonicated to obtain a stable suspension before fluorescence measurement.

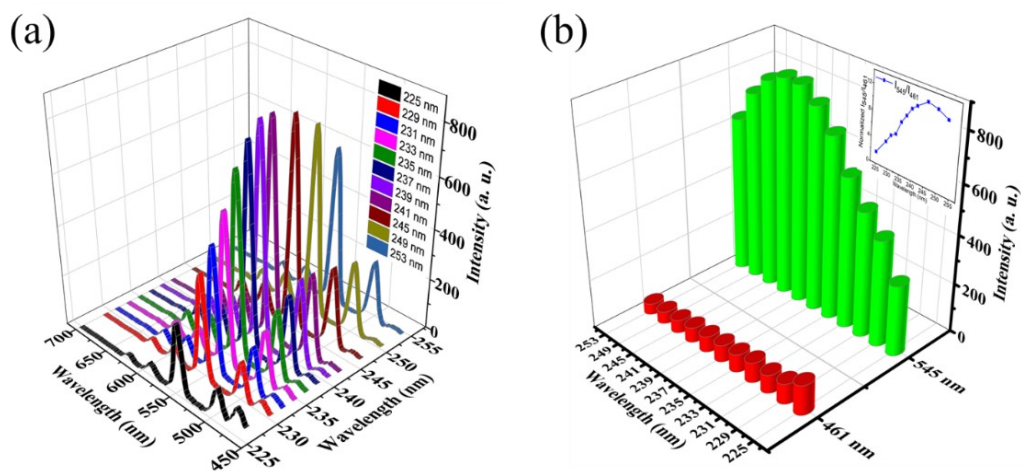


**Fig. S5.** (a) Emission spectra of the suspension of SiO<sub>2</sub>@Tb under the excitation from 225 to 253 nm. (b) Luminescence intensity of 545 nm and 461 nm of SiO<sub>2</sub>@Tb (inset: plot of the intensity ratio of I<sub>545</sub> and I<sub>461</sub> vs excitation wavelength).

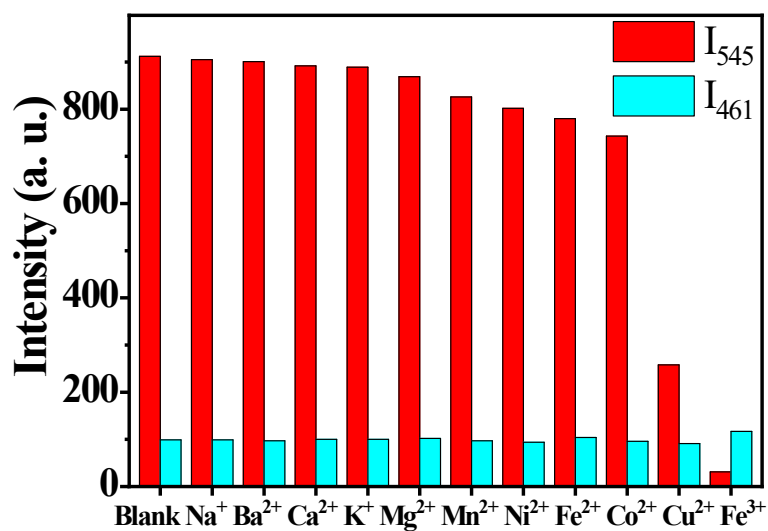


**Fig. S6.** Luminescence intensity of 545 nm and 461 nm of SiO<sub>2</sub>@Tb upon the addition of various metal ions under excitation at 237 nm.

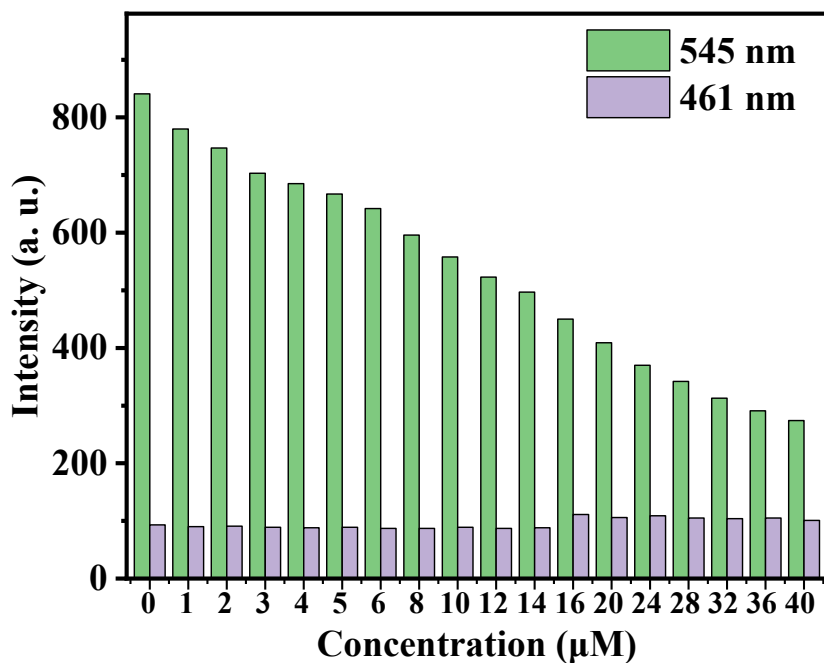


Fig. S7. Luminescence intensity of 545 nm and 461 nm of SiO<sub>2</sub>@Tb upon gradual addition of Cu<sup>2+</sup> ions under excitation at 237 nm (0-40 μM).

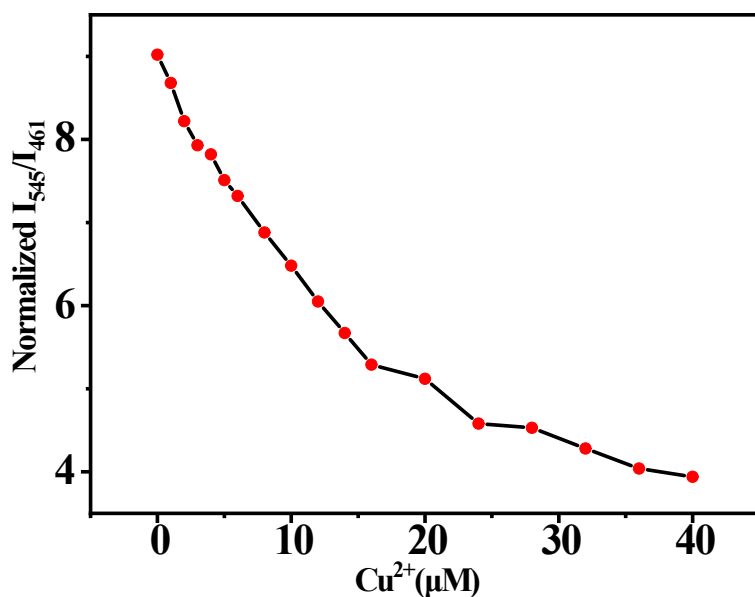
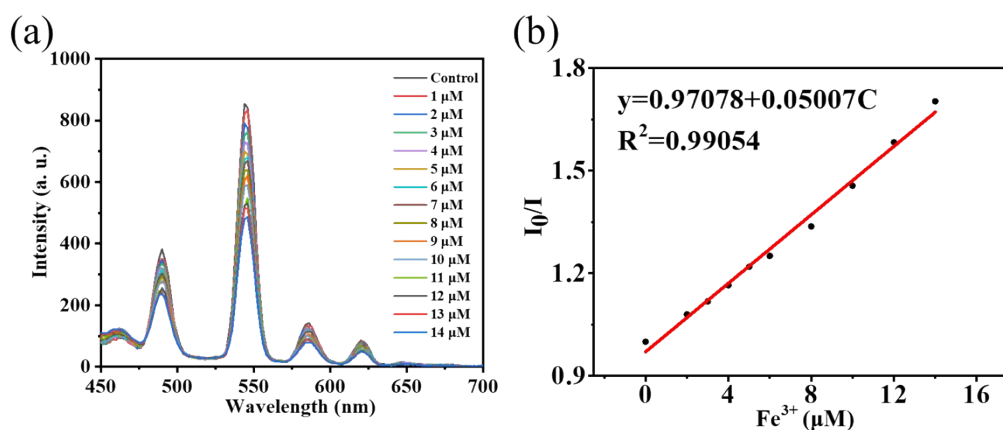
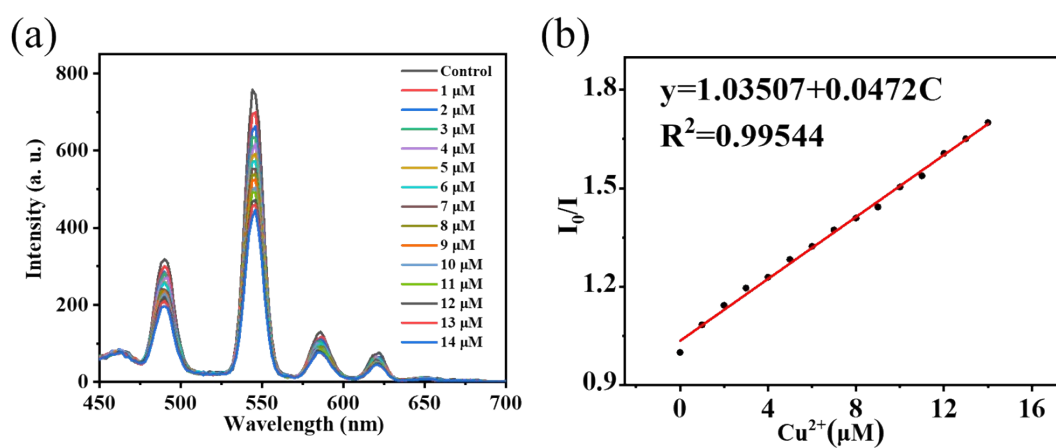


Fig. S8. Intensity ratio of I<sub>545</sub>/I<sub>461</sub> vs Cu<sup>2+</sup> ions concentration in the range of 0-40 μM.



**Fig. S9.** (a) Photoluminescence spectra ( $\lambda_{\text{ex}} = 237 \text{ nm}$ ) and (b) the corresponding Stern–Volmer plots of the suspension of  $\text{SiO}_2@\text{Tb}$  upon progressive addition of  $\text{Fe}^{3+}$  aqueous solution (0-14  $\mu\text{M}$ )



**Fig. S10.** (a) Photoluminescence spectra ( $\lambda_{\text{ex}} = 237 \text{ nm}$ ) and (b) the corresponding Stern–Volmer plots of the suspension of  $\text{SiO}_2@\text{Tb}$  upon progressive addition of the  $\text{Cu}^{2+}$  aqueous solution (0-14  $\mu\text{M}$ ).

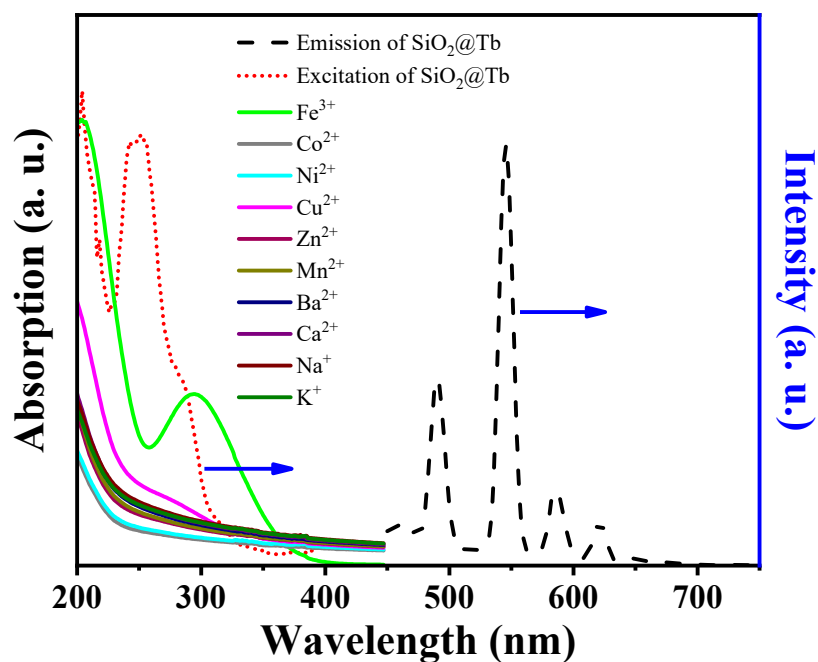


**Fig. S11.** Fluorescent excitation spectrum (Dotted line) and emission spectrum (Dashed line) of the suspension of  $\text{SiO}_2@\text{Tb}$  and the absorption spectra of various metal ions (Solid line).

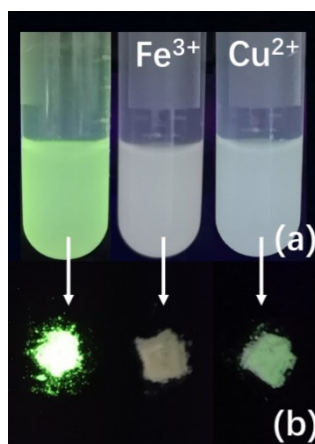


**Fig. S12.** Optical images of (a)  $\text{SiO}_2@\text{Tb}$  suspension before and after treatment with  $\text{Fe}^{3+}$  and  $\text{Cu}^{2+}$  ion under a UV lamp (from left to right,  $\lambda = 254 \text{ nm}$ ) and (b) corresponding images of  $\text{SiO}_2@\text{Tb}$  nanocomposites in dry solid state.

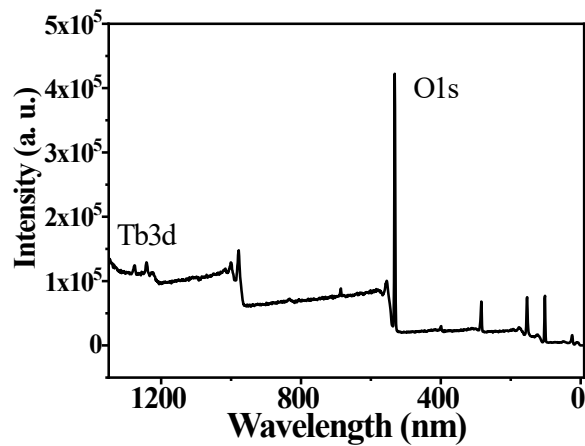


Fig. S13. XPS spectrum of SiO<sub>2</sub>@Tb.

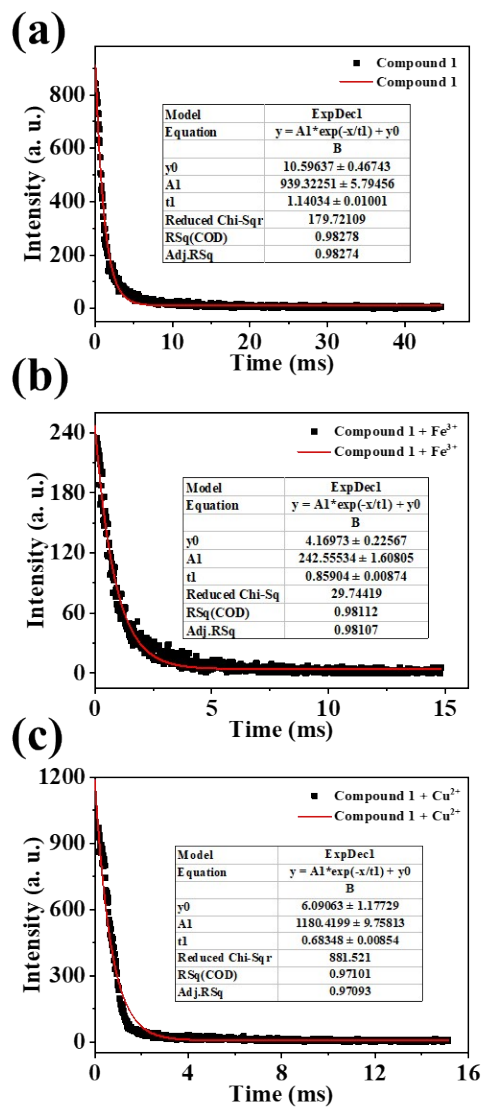


Fig. S14. Decay curves for Tb<sup>3+</sup> <sup>5</sup>D<sub>4</sub> → <sup>7</sup>F<sub>5</sub> emission in aqueous dispersion of SiO<sub>2</sub>@Tb (a) and treated with Fe<sup>3+</sup> (b) and Cu<sup>2+</sup> (c).

**Table S1** Sensitivity of various nanosensors for detection of Fe<sup>3+</sup>

	Materials	Probe	LOD	FL Ratios	Refs.
1	HPEI-CDs	Dual emission probe	0.47 μM	I <sub>321</sub> /I <sub>382</sub>	[1]
2	C-dots	Dual emission probe	0.16 μM	I <sub>350</sub> /I <sub>570</sub>	[2]
3	C-dots	single emission probe	1.68 μM	\	[3]
4	NS-CDs	Dual emission probe	0.56 μM	I <sub>480</sub> /I <sub>650</sub>	[4]
5	B-CQD/CdTe–Eu <sup>3+</sup>	Dual emission probe	0.053 μM	I <sub>410</sub> /I <sub>530</sub>	[5]
6	Neo-CDs	single emission probe	0.854 μM	\	[6]
7	R6G-CD	Dual emission probe	0.727 μM	I <sub>550</sub> /I <sub>455</sub>	[7]
8	GN-CDs	Dual emission probe	0.8 μM	I <sub>470</sub> /I <sub>570</sub>	[8]
9	SiO <sub>2</sub> @Tb	Dual emission probe	0.75 μM	I <sub>545</sub> /I <sub>461</sub>	This work

- [1] Wang B, Zhou X, Lin J, et al. Concentration-modulated dual-excitation fluorescence of carbon dots used for ratiometric sensing of Fe<sup>3+</sup>. *Microchemical Journal*, 2021, 164: 106028.
- [2] An Q, Lin Q, Huang X, et al. Electrochemical synthesis of carbon dots with a Stokes shift of 309 nm for sensing of Fe<sup>3+</sup> and ascorbic acid. *Dyes and Pigments*, 2021, 185:108878.
- [3] Peng Z. Sensitive, selective and reliable detection of Fe<sup>3+</sup> in lake water via carbon dots-based fluorescence assay. *Molecules*, 2022, 27(19): 6749.
- [4] Liang C, Xie X, Shi Q, et al. Nitrogen/sulfur-doped dual-emission carbon dots with tunable fluorescence for ratiometric sensing of ferric ions and cell membrane imaging. *Applied Surface Science*, 2022, 572: 151447.
- [5] Huang M, Tong C. A dual-emission ratiometric fluorescence probe for highly selective and simultaneous detection of tetracycline and ferric ions in environmental water samples based on a boron-doped carbon quantum dot/CdTe–Eu<sup>3+</sup> composite. *Environmental Science: Nano*, 2022, 9: 1712-1723.
- [6] Jadhav R W, Khobrekar P P, Bugde S T, et al. Nanoarchitectonics of neomycin-derived fluorescent carbon dots for selective detection of Fe<sup>3+</sup> ions. *Analytical Methods*, 2022,14: 3289-3298.
- [7] Deng M, Sha W, Liang C, et al. A FRET fluorescent nanosensor based on carbon dots for ratiometric detection of Fe<sup>3+</sup> in aqueous solution. *RSC Advances*, 2016, 6(32): 26936-26940.
- [8] Pang S, Liu S. Dual-emission carbon dots for ratiometric detection of Fe<sup>3+</sup> ions and acid phosphatase. *Analytica Chimica Acta*, 2020, 1105: 155-161.

**Table S2** Sensitivity of various nanosensors for detection of Cu<sup>2+</sup>

	Materials	Probe	LOD	FL Ratios	Refs.
1	GQD	Single emission probe	0.226 μM	\	[1]
2	AuNPs	Single emission probe	5.8 μM	\	[2]
3	Amino- CQDs	single emission probe	93 nM	\	[3]
4	Nitrogen-doped CQDs	single emission probe	0.16 μM	\	[4]
5	BSA-capped AuNCs	single emission probe	10 nM	\	[5]
6	NCDs	Dual emission probe	17.7 nM	I <sub>515</sub> /I <sub>454</sub>	[6]
7	Eu-DPA-CQDs	Single emission probe	6 nM	\	[7]
8	CQDs	Dual emission probe	0.076 μM	I <sub>562</sub> /I <sub>446</sub>	[8]
9	GSH@CDs-Au NCs	Dual emission probe	2.59 μM	I <sub>430</sub> /I <sub>700</sub>	[9]
10	MOF/ CdTe QDs	Dual emission probe	0.26 ng mL <sup>-1</sup>	I <sub>425</sub> /I <sub>605</sub>	[10]
11	QDC	Dual emission probe	34.9 nM	I <sub>430</sub> /I <sub>600</sub>	[11]
12	SiO <sub>2</sub> @Tb	Dual emission probe	0.91 μM	I <sub>545</sub> /I <sub>461</sub>	This work

- [1] Wang F, Gu Z, Lei W, et al. Graphene quantum dots as a fluorescent sensing platform for highly efficient detection of copper(II) ions. *Sensors and Actuators B: Chemical*, 2014, 190: 516-522.
- [2] Lin S, Liu S, Dai G, et al. A click-induced fluorescence-quenching sensor based on gold nanoparticles for detection of copper( II ) ion and ascorbic acid. *Dyes and Pigments*, 2021, 195: 109726.
- [3] Kalaiyarasan G, Joseph J. Efficient dual-mode colorimetric/fluorometric sensor for the detection of copper ions and vitamin C based on pH-sensitive amino-terminated nitrogen-doped carbon quantum dots: effect of reactive oxygen species and antioxidants. *Analytical and bioanalytical chemistry*, 2019, 411(12): 2619-2633.
- [4] Hu C, Zhu Y, Zhao X. On-off-on nanosensors of carbon quantum dots derived from coal tar pitch for the detection of Cu<sup>2+</sup>, Fe<sup>3+</sup>, and L-ascorbic acid. *Spectrochimica Acta Part A: Molecular and Biomolecular Spectroscopy*, 2021, 250: 119325.
- [5] Wu J, Jiang K, Wang X, et al. On-off-on gold nanocluster-based near infrared fluorescent probe for recognition of Cu(II) and vitamin C. *Microchimica Acta*,

- 2017, 184(5): 1315-1324.
- [6] Guo, J. Liu, A. Zeng, Y. et al. Novel dual-emission fluorescence carbon dots as a ratiometric probe for  $\text{Cu}^{2+}$  and  $\text{ClO}^-$  detection. *Nanomaterials* 2021, 11: 1232.
  - [7] Li Y, Liu D, Wang Y Q, et al.  $\text{Eu}^{3+}$ -functionalized CQD hybrid material: synthesis, luminescence properties and sensing application for the detection of  $\text{Cu}^{2+}$ . *Materials Advances*, 2021, 2: 3346-3352.
  - [8] Han Z, Nan D, Yang H, et al. Carbon quantum dots based ratiometric fluorescence probe for sensitive and selective detection of  $\text{Cu}^{2+}$  and glutathione. *Sensors and Actuators B: Chemical*, 2019, 298: 126842.
  - [9] Wu J, Li R, Liu S. A novel dual-emission fluorescent probe for ratiometric and visual detection of  $\text{Cu}^{2+}$  ions and  $\text{Ag}^+$  ions. *Analytical and Bioanalytical Chemistry*, 2022, 414(9): 3067-3075.
  - [10] Yang Y, Liu W, Cao J, et al. On-site, rapid and visual determination of  $\text{Hg}^{2+}$  and  $\text{Cu}^{2+}$  in red wine by ratiometric fluorescence sensor of metal-organic frameworks and CdTe QDs. *Food Chemistry*, 2020, 328 127119.
  - [11] Manna M, Roy S, Bhandari S, et al. A dual-emitting quantum dot complex nanoprobe for ratiometric and visual detection of  $\text{Hg}^{2+}$  and  $\text{Cu}^{2+}$  ions. *Journal of Materials Chemistry C*, 2020, 8(21): 6972-6976.